

1 **Spatially explicit global hotspots driving China's**
2 **mercury related health impacts**

3 Yumeng Li ^{1,#}, Long Chen ^{2,#}, Sai Liang ^{3,1,*}, Jianchuan Qi ^{3,1}, Haifeng Zhou ¹,
4 Cuiyang Feng ¹, Xuechun Yang ¹, Xiaohui Wu ¹, Zhifu Mi ⁴, Zhifeng Yang ^{3,5}

5 ¹ State Key Joint Laboratory of Environment Simulation and Pollution Control,
6 School of Environment, Beijing Normal University, Beijing, 100875, P. R. China

7 ² Key Laboratory of Geographic Information Science (Ministry of Education), School
8 of Geographic Sciences, East China Normal University, Shanghai, 200241, P. R.
9 China

10 ³ Key Laboratory for City Cluster Environmental Safety and Green Development of
11 the Ministry of Education, Institute of Environmental and Ecological Engineering,
12 Guangdong University of Technology, Guangzhou, Guangdong, 510006, P. R. China

13 ⁴ The Bartlett School of Construction and Project Management, University College
14 London, London, WC1E 7HB, UK

15 ⁵ Guangdong Provincial Key Laboratory of Water Quality Improvement and
16 Ecological Restoration for Watersheds, Institute of Environmental and Ecological
17 Engineering, Guangdong University of Technology, Guangzhou, 510006, People's
18 Republic of China

19 # These two authors contributed equally.

20 * Corresponding author: liangsai@gdut.edu.cn (Sai Liang).

21 **ABSTRACT**

22 Over 100 nations signed the *Minamata Convention on Mercury* to control the adverse
23 effects of mercury (Hg) emissions on human beings. A spatially explicit analysis is
24 needed to identify the specific sources and distribution of Hg-related health impacts.
25 This study maps China's Hg-related health impacts and global supply chain drivers
26 (i.e., global final consumers and primary suppliers) at a high spatial resolution. Here
27 we show significant spatial heterogeneity in hotspots of China's Hg-related health
28 impacts. Approximately 1% of the land area holds only 40% of the Chinese
29 population but nearly 70% of the fatal heart attack deaths in China. Moreover,
30 approximately 3% of the land area holds nearly 60% of the population but 70% of the
31 intelligence quotient (IQ) decrements. The distribution of hotspots of China's
32 Hg-related health impacts and global supply chain drivers are influenced by various
33 factors including population, economy, transportation, resources, and dietary intake
34 habits. These spatially explicit hotspots can support more effective policies in various
35 stages of the global supply chains and more effective international cooperation to
36 reduce Hg-related health impacts. This can facilitate the successful implementation of
37 the *Minamata Convention on Mercury*.

38

39 **KEYWORDS**

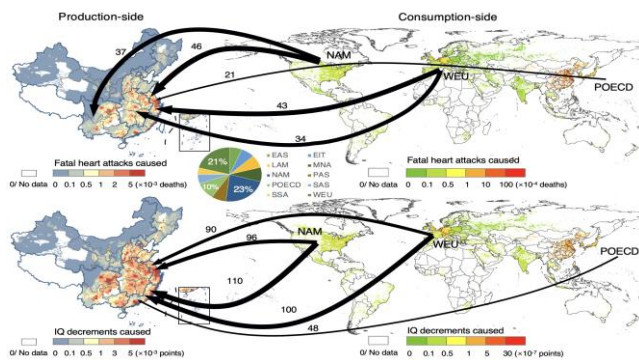
40 Mercury; health impacts; supply chain; input-output analysis; spatially explicit
41 analysis; trade; footprint; Minamata Convention

42 **SYNOPSIS**

43 Spatially explicit analyses for China’s Hg-related health impacts and relevant global
44 economic drivers can facilitate the smooth implementation of the Minamata
45 Convention on Mercury.

46

47 **GRAPHICAL ABSTRACT/ TOC**



48

49

50 **1. INTRODUCTION**

51 Mercury (Hg) is a global pollutant that can be transported worldwide and is
52 difficult to be removed from the environment.^{1, 2} One of its forms, methylmercury
53 (MeHg), is highly toxic to the nervous, digestive, and immune systems of human
54 body, as well as the development of the child in utero.^{3, 4} Given the adverse impacts of
55 Hg on human beings, the World Health Organization (WHO) has listed Hg as one of
56 the top ten chemicals with primary public health concern.³ To control global
57 anthropogenic Hg emissions and their adverse effects on human beings, over 100
58 nations signed the *Minamata Convention on Mercury (Minamata Convention)*⁵. This

59 convention entered into force on 16 August 2017, which is the first global agreement
60 to protect human health and the environment in the recent decade.⁶

61 In order to reduce the human health damage of global Hg pollution, lots of studies
62 have been conducted to evaluate Hg-related health impacts via MeHg intake and
63 dose-response relationship of MeHg exposure.^{7,8} Studies on prenatal MeHg exposure
64 indicate that MeHg intake can have severe impacts on neurodevelopment in children,
65 thus affecting their intelligence quotient (IQ) and cognitive levels.⁹ In addition, MeHg
66 exposure is closely associated with the risks of cardiovascular diseases.¹⁰ Given the
67 long-distance transport of Hg, the assessment of Hg-related health impacts should be
68 based on a complete Hg cycle (e.g., atmospheric Hg emissions¹¹⁻¹³, atmospheric Hg
69 transport and deposition^{14, 15}, MeHg bioaccumulation^{4, 16}, and Hg-related health risks<sup>17,
70 18</sup>). Recently, studies have combined the economic systems with traditional
71 biogeochemical Hg cycle to identify the impacts of economic activities and
72 international trade on Hg emissions and related health impacts. For example, previous
73 studies have characterized the impacts of local Hg emissions on domestic human
74 health in the U.S and China.^{17, 19,20} In addition to local Hg emissions, remote economic
75 activities can also influence local Hg emissions through global supply chains^{17,21,22} and
76 subsequently influence human health^{13,17,18}. For instance, our recent study has revealed
77 China's regional Hg-related health impacts driven by the economic activities of other
78 regions in China.¹⁷ In addition to domestic economic drivers, international economic
79 activities also influence domestic Hg-related health impacts via global supply chains.
80 This requires international cooperation which is an important component of the

81 *Minamata Convention*⁵. However, the global economic drivers (including global final
82 consumers and primary suppliers) of local Hg-related health impacts have not been
83 well characterized yet.

84 Moreover, Hg-related health impacts and economic activities are both highly
85 localized and have significant spatial heterogeneity.²³ Existing studies have nationally
86 or sub-nationally averaged out the spatial characteristics of Hg-related health impacts
87 and economic activities.^{17, 19} However, they ignored the identification of Hg-related
88 health impacts and economic drivers at a high spatial resolution. It is important to
89 develop a highly resolved inventory to explicitly spatialize the supply chain hotspots
90 of Hg-related health impacts (including the occurrence of Hg-related health impacts,
91 global final consumers, and global primary suppliers). This effort can more accurately
92 locate the hotspots for Hg control measures and effectively facilitate the
93 implementation of the *Minamata Convention*.

94 This study fulfils the above knowledge gaps, taking China as a representative case.
95 China is important in global biogeochemical Hg cycle due to its largest atmospheric
96 Hg emissions and population in the world.²⁴ Atmospheric Hg deposition over China
97 has been proven to adversely affect human health through the intake of Hg-containing
98 foods (e.g., rice, fish, vegetables, and meat).^{25, 26} The MeHg intake has resulted in
99 approximately 0.14 points of per-foetus IQ decrements and 7,360 deaths from fatal
100 heart attacks in China in 2010.¹⁷ Moreover, China participates in intensive trade of
101 commodities with other nations and plays the role of world factory in global supply

102 chains.²⁷ Identifying the hotspots for China's Hg-related health impacts and global
103 supply chain drivers plays an important role in global Hg control.

104 To effectively identify the global supply chain hotspots driving China's
105 Hg-related health impacts at a high spatial resolution, this study constructs a model
106 for the Spatially Explicit Global Tracking of Hg-related Health Impacts (SEGTHI).
107 This model integrates global economic supply chains with China's biogeochemical Hg
108 cycle to track spatially explicit hotspots of global supply chains driving the spatially
109 explicit health impacts of China's Hg emissions. We map China's Hg-related health
110 impacts (including IQ decrements and deaths from fatal heart attacks) in 2010 caused
111 by local production, global final demand, and global primary inputs at a high spatial
112 resolution. In this way, we can identify key hotspots of Hg-related health impacts and
113 global supply chain drivers at a finer scale than the national and sub-national levels.
114 These findings can facilitate distinct Hg control strategies and international
115 cooperation to reduce Hg-related health impacts more effectively. It is worth noting
116 that there is a time lag between MeHg intake and the response of heart attacks
117 (generally 6 years). Moreover, the data on population structure (i.e., the Sample
118 Survey Data of 1% of National Population²⁸) used to calculate the fatal heart attack
119 deaths are only updated to 2015. Consequently, we use the global MRIO data in 2010
120 and estimate China's Hg-related health impacts in 2010.

121 **2. METHODS AND DATA**

122 The SEGTHI model consists of three components, including (1) the global
123 environmentally extended multi-regional input-output (EE-MRIO) model, (2) the
124 biogeochemical Hg cycle, and (3) the spatially explicit mapping for Hg-related health
125 impacts of China caused by domestic production, global final demand, and global
126 primary inputs. This study evaluates the roles of 30 Chinese provinces and 140
127 nations as primary suppliers, direct emitters, and final consumers for China's
128 Hg-related health impacts at a high spatial resolution. Tables S1 and S2 in the
129 Supporting Information (SI) present the list of Chinese provinces, world nations, and
130 aggregated regions. The framework of the SEGTHI model in this study is illustrated
131 in Figure S1. Here we provide the simplified methods and the detailed methods and
132 data can be found in section S1 of the SI.

133 **2.1 Global EE-MRIO model**

134 We use the global EE-MRIO model to evaluate the roles of nations and Chinese
135 provinces as primary suppliers, direct emitters, and final consumers for atmospheric
136 Hg emissions in China. The global EE-MRIO model has been widely used to
137 investigate environmental issues related to interregional trade, such as resource
138 extraction²⁹ and atmospheric emissions^{27,30,31}. The global EE-MRIO model is
139 constructed with a global multi-regional input-output (MRIO) table and a satellite
140 account of environmental issues (i.e., atmospheric Hg emissions in China in this
141 study). This model is used to calculate production-based, consumption-based, and
142 income-based emissions of nations and Chinese provinces for atmospheric Hg
143 emissions in China. We use the Chinese atmospheric Hg emission inventory compiled

144 in our previous work¹⁴ to construct the satellite account of the global EE-MRIO model.
145 The atmospheric Hg emission inventory is compiled by multiplying energy uses or
146 product yields with corresponding emission factors.¹⁴ The global MRIO table is
147 constructed by Mi et al.³², which links the Chinese MRIO data to the Global Trade and
148 Analysis Project (GTAP) database. The base year in this study is set as 2010.

149 The production-based Hg emissions are direct geographic Hg emissions from the
150 physical emitters. They are the satellite account of the global EE-MRIO table. We
151 define the Hg emission intensity of each sector using Eq. (1).

152

153 The notation E_n indicates production-based Hg emissions of sectors in province n .
154 The row vector q indicates the direct Hg emission intensity of each province sector,
155 which represents Hg emissions for unitary output of each province sector. The column
156 vector y_n represents the total output of sectors in province n .

157 Consumption-based Hg emissions of nations and Chinese provinces are calculated
158 by the Leontief MRIO model, which regards the economy as demand-driven.
159 Consumption-based Hg emissions represent China's Hg emissions directly and
160 indirectly driven by the final demand of nations and Chinese provinces^{31, 33}, as shown
161 in Eq. (2).

162

163 The notation E_n represents consumption-based Hg emissions of nation/province n .
164 The row vector q indicates the direct Hg emission intensity of each province sector.

165 The column vector d_n represents the final demand of nation/province n . The matrix A is
166 the direct input coefficient matrix, in which each element a_{ij} equals to direct input from
167 sector i to sector j divided by the total output of sector j . The matrix I is an identify
168 matrix. The matrix L is the Leontief Inverse matrix, which describes both direct and
169 indirect inter-sectoral relationships of the outputs and unitary final demand³⁴.

170 Income-based Hg emissions of nations and Chinese provinces are calculated by
171 the Ghosh MRIO model, which regards the economy as supply-push. Income-based
172 Hg emissions represent China's Hg emissions directly and indirectly enabled by
173 primary inputs of nations and Chinese provinces^{35, 36}, as shown in Eq. (3).

174

175 The notations e_n represents income-based Hg emissions of nation/province n . The
176 row vector p_n indicates the primary inputs of nation/province n (values for sectors of
177 nation/province n are non-zero and values for other nation/province sectors are zeros).
178 The column vector q' represents the transposition of the Hg emission intensity vector
179 q . The matrix B is the direct output coefficient matrix, in which each element b_{ij} equals
180 to direct input from sector i to sector j divided by the total output of sector i . With an
181 identity matrix I , the matrix G is the Ghosh Inverse matrix, which represents both
182 direct and indirect inter-sectoral relationships of the outputs and unitary primary
183 inputs.³⁴

184 **2.2 Biogeochemical cycle of Hg**

185 The methods for modelling the biogeochemical cycle of Hg in this study refer to
186 those in our previous work¹⁷. Here we give a brief overview of each component, while
187 specific methods are described in SI S1.2. We also provided the details on related
188 methods and data on our website (<https://www.cgeed.net/cmstm-model>). The
189 biogeochemical cycle of Hg consists of five components which occur over mainland
190 China and the coastal seas, including a Chinese anthropogenic Hg emission inventory,
191 an atmospheric transport model, changes in food MeHg resulting from atmospheric
192 deposition, a human intake inventory of MeHg, and human health impacts due to
193 MeHg intake. Meanwhile, two external components include Hg emissions from
194 natural sources and foreign anthropogenic sources, and imports of food products from
195 foreign nations.

196 We use the Chinese atmospheric Hg emissions inventory compiled in our previous
197 work as the production-based emission inventory.¹⁴ The production-based emissions
198 are distributed as point and non-point sources, which serve as the input of an
199 atmospheric transport model. Then, we use the GEOS-Chem chemical transport
200 model (version 9-02; <http://geos-chem.org>) to simulate atmospheric Hg cycle over
201 China. A nested simulation at a horizontal resolution of $1/2^\circ \times 2/3^\circ$ over China is
202 conducted in a boundary condition provided by a global simulation at a horizontal
203 resolution of $4^\circ \times 5^\circ$. Changes in Hg deposition simulated by the model are used as a
204 measure of changes in Hg concentrations in Hg-containing food products, including
205 ten categories of food products (i.e., rice, wheat, beans, vegetables, pork, poultry,
206 milk, eggs, marine fish, and freshwater fish) referred from previous studies^{25, 37}. Next,

207 we compile an intake inventory at the provincial scale to present a map of MeHg
208 intake for the population over China in the model. The data regarding the compilation
209 of intake inventory of MeHg and the evaluation of human health impacts are from our
210 previous study¹⁷. In addition to the intake inventory, the model involves the
211 dose-response relationships between dietary intake of MeHg and Hg-related health
212 impacts to evaluate the health impacts. The dose-response relationships referred to in
213 previous studies are based on epidemiological studies.^{10,19,38}

214 **2.3 Spatially explicit mapping**

215 The spatially explicit mapping of Hg-related health impacts in China includes the
216 impacts caused by domestic production, global final demand, and global primary
217 inputs. The grid maps of Hg-related health impacts in China caused by domestic
218 production show the occurrence of foetal IQ decrements and deaths from fatal heart
219 attacks. For grid maps of Hg-related health impacts in China caused by global final
220 demand and primary inputs, data in each grid represent the foetal IQ decrements and
221 deaths from fatal heart attacks occurring in China caused by the final demand and
222 primary inputs in this grid.

223 For Hg-related health impacts in China caused by domestic production, we use the
224 gridded food consumption expenditure data in China as the proxy to spatialize the
225 foetal IQ decrements and deaths from fatal heart attacks in China. Due to the lack of
226 basic gridded data, we multiply the per-capita food consumption expenditure data of
227 China at the city level with gridded population to obtain the gridded data for food

228 consumption. We select China's gridded population in 2010 and 2015 at the 1km ×
229 1km grid scale as the basic grid data, which are from the Institute of Geographic
230 Sciences and Natural Resources Research, Chinese Academy of Sciences³⁹. The
231 gridded population in 2010 is used in the evaluation of the foetal IQ decrements, and
232 the gridded population in 2015 is used to investigate Hg-related fatal heart attacks to
233 reflect the time lag between MeHg intake and the response of heart attacks.¹⁷ The
234 gridded population data are calibrated with the official demographic statistics^{40,28}.
235 Notably, when calculating the foetal IQ decrements, we multiply the birth rate in 2010
236 to the gridded population data to obtain the gridded data of new-born population. The
237 birth rate data can be obtained from the China Statistical Yearbook⁴⁰.

238 For grid maps of China's Hg-related health impacts driven by global final demand,
239 we construct a grid map for global final demand as the proxy to spatialize the health
240 impacts. The grid map for global final demand is constructed with the final demand of
241 nations and Chinese provinces in the global MRIO table and the global nighttime
242 lights data at the 1km × 1km grid scale in 2010. The grid data for global nighttime
243 lights can be obtained from the Defense Meteorological Satellite Program's
244 Operational Linescan System (DMSP-OLS) Nighttime Lights Time Series⁴¹. They can
245 directly reflect the intensity of human activities and describe the socioeconomic
246 development level of a region.⁴² We simulated the relationship between the global
247 final demand and the values of nighttime lights. We observed a significant positive
248 correlation relationship between them, and the fitting degree is high (SI Figure S5).
249 Therefore, we assume that the spatial distribution of nighttime lights is consistent with

250 that of the final demand. Subsequently, we use the values of nighttime lights at the
251 1km × 1km grid scale as the proxy variable to spatialize global final demand at the
252 national/subnational scale. In this way, we can investigate global final consumers
253 driving China's Hg-related health risks at a higher spatial resolution to support more
254 targeted policy decisions.

255 The primary inputs are also called value added, whose sum in each region is equal
256 to the Gross Domestic Product (GDP). The main variable that influences the primary
257 inputs is GDP. Thus, for grid maps of Hg-related health impacts in China enabled by
258 global primary inputs, we use the global gridded GDP data at the 1km × 1km scale
259 in 2010 developed by United Nations Environment Programme⁴³ as the proxy variable
260 to spatialize the health impacts. See section S1.3 of the SI for specific methods.

261 **3. RESULTS AND DISCUSSION**

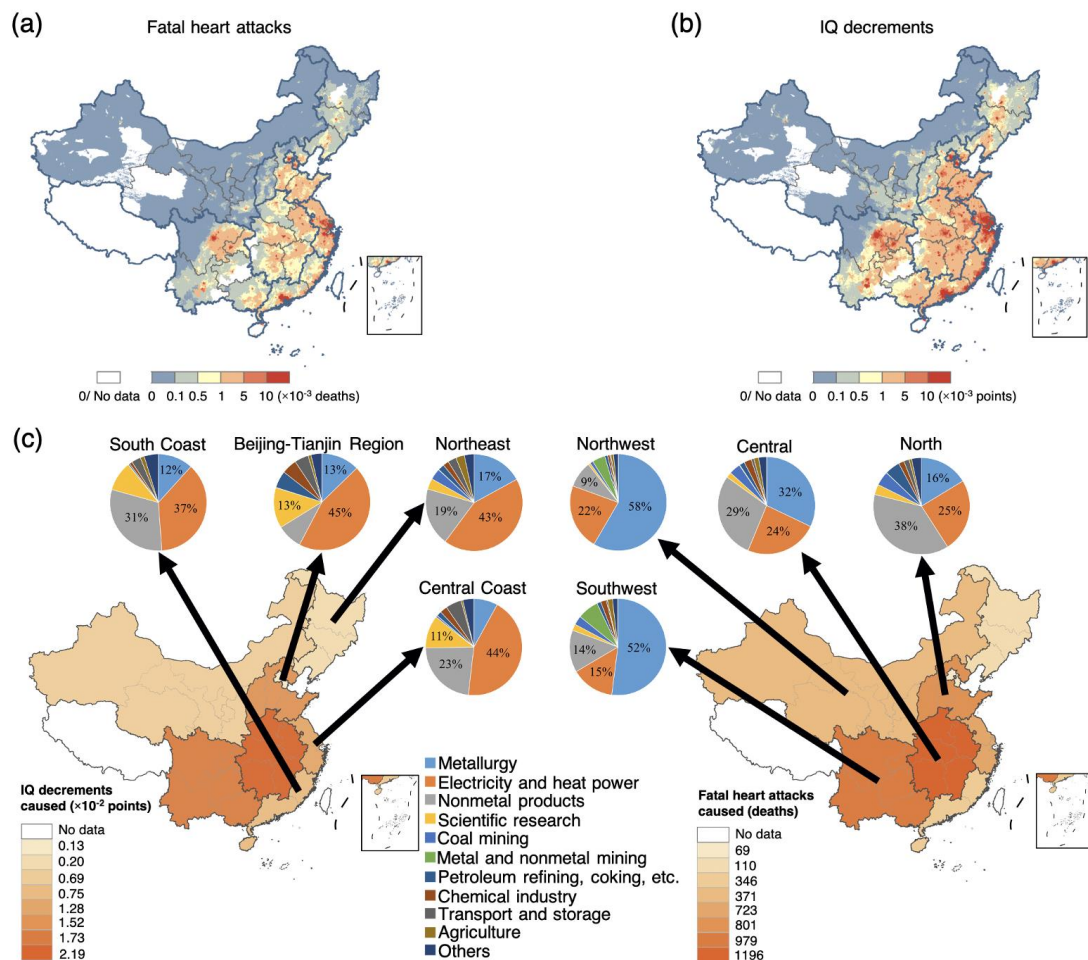
262 **3.1 Spatially explicit health impacts of atmospheric Hg emissions in China**

263 Overall, anthropogenic atmospheric Hg emissions in China led to 8.48×10^{-2} points
264 of per-foetus IQ decrements and 4,593 deaths from fatal heart attacks in 2010. These
265 impacts generally increase from northwestern inland areas to southeastern coastal
266 areas (Figure 1a-b). Figure 1c shows that atmospheric Hg emissions of Central China
267 lead to the most national health impacts, with 2.19×10^{-2} points of per-foetus IQ
268 decrements and 1,196 deaths from fatal heart attacks. In terms of sectoral sources, the
269 electricity and heat power sector is the major sectoral source of national Hg-related
270 health impacts in eastern regions (including the Northeast, Beijing-Tianjin Region,
271 Central Coast, and South Coast), contributing approximately 40% in each region. The

272 metallurgy industry plays a dominant role in western regions, including the Northwest
273 and Southwest. In addition, for the North and Central, the nonmetal products,
274 metallurgy, and electricity and heat power sectors are all important sources of national
275 Hg-related health impacts. Specially, a significant spatial heterogeneity was observed
276 in hotspots of China's Hg-related health impacts. Approximately 1% of the land area
277 holds 40% of the Chinese population but nearly 70% of the deaths from fatal heart
278 attacks in China. Moreover, approximately 3% of the land area holds nearly 60% of
279 the Chinese population but 70% of the IQ decrements. For example, approximately 80%
280 of the hotspots in Sichuan Province are located in the Chengdu-Chongqing District
281 (occupying only 32% of the land area in Sichuan) of eastern Sichuan. Few hotspots
282 have been observed in western Sichuan because western Sichuan is mountainous with
283 lower population and less industrial activities. This indicates the necessity of spatially
284 explicit mapping to accurately identify the hotspots and effectively reduce Hg-related
285 health impacts in China. Moreover, it shows that the hotspots of economic activities
286 and Hg-related health impacts are driven by various factors, not just the population
287 density.

288 The spatial distribution of Hg-related health impacts is affected by many factors,
289 including population, economy, resources, and dietary intake habits. Many hotspots of
290 Hg-related health impacts are distributed in urban agglomerations. This pattern is the
291 most obvious in the Yangtze River Delta (including Shanghai, South Jiangsu, North
292 Zhejiang, and some regions in Anhui), Beijing-Tianjin-Hebei Region, Pearl River
293 Delta (including Guangzhou, Foshan, Shenzhen, and Zhuhai in Guangdong Province),

294 and Chengdu-Chongqing District. For example, the land area of the Yangtze River
 295 Delta and Pearl River Delta urban agglomerations accounts for only 4% of the whole
 296 country, but holds approximately 30% of China's Hg-related health impacts. Most of
 297 these cities are provincial capitals or municipalities, such as Beijing, Shanghai,
 298 Nanjing, Hangzhou, Guangzhou, and Chengdu (see SI Figure S5a for provincial
 299 boundaries). These cities have large populations and high levels of socioeconomic
 300 development, inducing large amounts of anthropogenic Hg emissions. Meanwhile,
 301 their populations consume large amounts of marine fish and meat with relatively high
 302 Hg concentration. This subsequently results in high Hg-related health impacts in these
 303 cities.



304

305 **Figure 1. Spatially explicit human health impacts caused by anthropogenic**
306 **atmospheric Hg emissions in China in 2010.** Graphs *a* and *b* describe spatially
307 explicit deaths from fatal heart attacks due to methylmercury intake and total foetus
308 IQ decrements in each grid. It is worth noting that graph *b* shows the total IQ
309 decrements for the total new-born population in each grid. Graph *c* shows national
310 per-foetus IQ decrements and deaths from fatal heart attacks caused by anthropogenic
311 atmospheric Hg emissions in each region of China. The pie chart shows the
312 contributions of sectors in each region to the national health impacts caused by
313 atmospheric Hg emissions in this region.

314

315 Moreover, parts of the hotspots of China's Hg-related health impacts are
316 associated with the distribution characteristics of mineral and water resources. China's
317 mineral resources are mainly distributed in the North, Northwest, and Southwest,⁴⁴
318 where many hotspots of Hg-related health impacts are located. Famous metal mining
319 areas include iron mines in Panzhihua of Sichuan, Hg mines in Tongren of Guizhou,
320 and gold mines in Zhaoyuan of Shandong (SI Figure S5b). For fossil fuels, Shanxi,
321 Xinjiang, and Sichuan are the major producers of coal, oil, and natural gas,
322 respectively. These resource-abundant areas discharge large amounts of atmospheric
323 Hg emissions due to intensive mining, smelting, and energy combustion activities.
324 This subsequently results in significant Hg-related health impacts. Figure 1c shows
325 that the *metallurgy* industry is an important source of national Hg-related health
326 impacts for these resource-based regions, including the Northwest (58%), Southwest
327 (52%), and North China (16%). In addition to mineral resources, Hg-related health
328 impact hotspots are also associated with water resources because water resources are
329 essential for industrial production.⁴⁵ For instance, many hotspots are located in areas

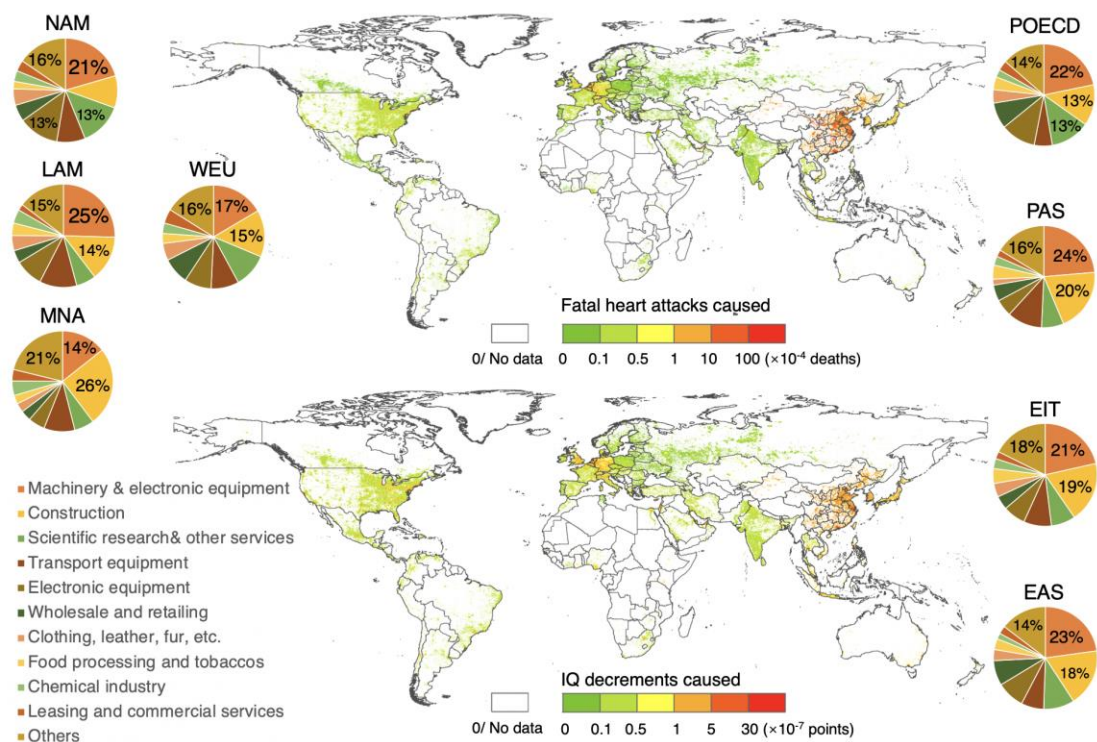
330 of the Yellow River catchment across the Gansu, Ningxia, and Shanxi provinces (SI
331 Figure S5b). Moreover, Hg-related health impacts in southeast coastal areas are
332 generally higher than other areas. This situation might be related to the higher
333 consumption of fish, because fish consumption is a major pathway of MeHg
334 exposure³⁷.

335 **3.2 Spatially explicit global final consumers driving Hg-related health impacts**

336 Domestic consumption (mainly in Central China, Central Coast China, and
337 Northwest China) contributes 82% of the Hg-related health impacts in China, while
338 foreign consumption (mainly in North America, Western Europe, Japan, India, and
339 the Middle East) contributes the remaining 18% of impacts (see SI Figure S6 for
340 details of domestic and foreign consumers). The U.S. is the largest foreign consumer,
341 contributing 3.2×10^{-3} points of per-foetus IQ decrements and 171 deaths from fatal
342 heart attacks. At the sectoral level, domestic demand of construction activities is the
343 largest source. In most foreign regions, the consumption of mechanical and electrical
344 products is the largest source (contributing over 20%). However, in the Middle East
345 and North Africa, the final demand of construction activities has the leading role
346 (contributing 25%). The demand for building materials (e.g., cement, steel, and
347 ceramic tiles) in the Middle East (especially Saudi Arabia) is highly dependent on
348 China.⁴⁶

349 Figure 2 shows a significant spatial heterogeneity in global consumers driving
350 Hg-related health impacts in China. The consumption activities in approximately 0.1%

351 of the global land area holds nearly 10% of the global population but drives 70% of
352 the Hg-related health impacts in China. Overall, the domestic consumption in China
353 has driven the majority of China's Hg-related health impacts. Since domestic hotspots
354 in China are much larger than other global hotspots, we have adopted another
355 classification to obtain more details about hotspots in China (SI Figure S7). The
356 hotspots in China are mainly concentrated in North China, South Coast China,
357 Middle-Lower Yangtze Region, and Pearl River Delta. They are the most developed
358 regions in China with large populations and intensive consumption activities. They
359 drive large Hg-related health impacts in China through global supply chains. The
360 details are shown in the section S2 of the SI for the consumption of specific Chinese
361 regions driving China's Hg-related health impacts. In addition, we observe significant
362 influences of transportation and resources on the distribution of hotspots, mainly in
363 developing areas (e.g., Yunnan, Guizhou, Guangxi, Eastern Sichuan, and the Yellow
364 River Basin). These hotspots distribute along roads and rivers.



365

366 **Figure 2. Spatially explicit global consumers driving China's Hg-related health**
 367 **impacts in 2010.** Abbreviations: NAM – North America; LAM – Latin America and
 368 the Caribbean; WEU – Western Europe; MNA – the Middle East and North Africa;
 369 PAS – Southeast Asia and the Pacific; POECD – Pacific-OECD-1990 nations
 370 (including Japan, Australia, and New Zealand); EIT – Economies in Transition
 371 (including Eastern Europe and the former Soviet Union); EAS – East Asia (China
 372 excluded).

373

374 Foreign consumers driving China's Hg-related health impacts mainly include the
 375 U.S., Western Europe, Japan, and South Korea (See section S2 of the SI for more
 376 international pairs). They are developed nations and regions, where the hotspot
 377 locations are based on urban agglomerations centred on large cities. Cities are
 378 aggregation areas of consumption activities. They consume large amounts of
 379 commodities that directly and indirectly lead to atmospheric Hg emissions and related
 380 health impacts in China. For instance, in the eastern U.S., hotspots are concentrated in

381 the megalopolises of New York, Boston, Washington D.C., Atlanta, and Chicago,
382 forming a dotted distribution. The consumption of mechanical and electrical products
383 in these regions results in significant Hg-related health impacts in China through
384 global supply chains (Figure 2). In Western Europe, the consumption of Netherlands,
385 Belgium, western Germany, and southern United Kingdom leads to the most
386 Hg-related health impacts in China. In addition, some regions in Southeast Asia (e.g.,
387 Hanoi and Ho Chi Minh City in Vietnam, Bangkok in Thailand, Kuala Lumpur in
388 Malaysia, and Singapore) have close trade ties with China. Their consumption has
389 driven large Hg-related health impacts in China.

390 The transportation is also an important factor affecting the distribution of global
391 consumers driving China's Hg-related health impacts. This distribution feature is
392 mainly manifested as a coastal distribution. The geographical location of coastal areas
393 facilitates international trade activities. For example, consumption hotspots on the
394 west and east coast of the U.S., the west coast of Latin America and Caribbean, and
395 the south coast of West Africa all follow the coastal distribution patterns. Another
396 typical area of the transportation-based pattern is the Mid-Eastern of the U.S. There
397 are major cities working as freight transportation nodes, and the hotspots are radiantly
398 distributed on the dominating transportation arteries. For example, the Ohio state
399 ranks second among all the U.S. states in terms of China's Hg-related health impacts
400 driven by the final demand of various states in the U.S. However, the total value of
401 Ohio's nighttime lights ranks only 7th. There are not too many nighttime lights in
402 Ohio, but China's Hg-related health impacts caused by its final demand are high. One

403 possible reason is the influence of transportation factors. As the third most developed
404 state in manufacturing in the U.S., Ohio plays an important role as freight
405 transportation hub.⁴⁷ For instance, the freight volume on the Ohio River is twice that
406 of the Panama Canal.⁴⁸ Another area worthy of attention is Minnesota (especially
407 Minneapolis and St. Paul). It ranks sixth among all the U.S. states in terms of China's
408 Hg-related health impacts driven by the final demand of various states in the U.S.
409 However, its population only ranks 21st among the U.S. states. Minnesota is adjacent
410 to the Great Lakes and Mississippi River. It also borders Canada. This makes it an
411 important port and rail transportation center.⁴⁸ These findings indicate that particular
412 areas responsible for high Hg-related health impacts are not necessarily big cities with
413 large populations or nighttime lights. Convenient traffic conditions can also make
414 final demand activities gather here, resulting in high Hg-related health impacts in
415 China through global supply chains.

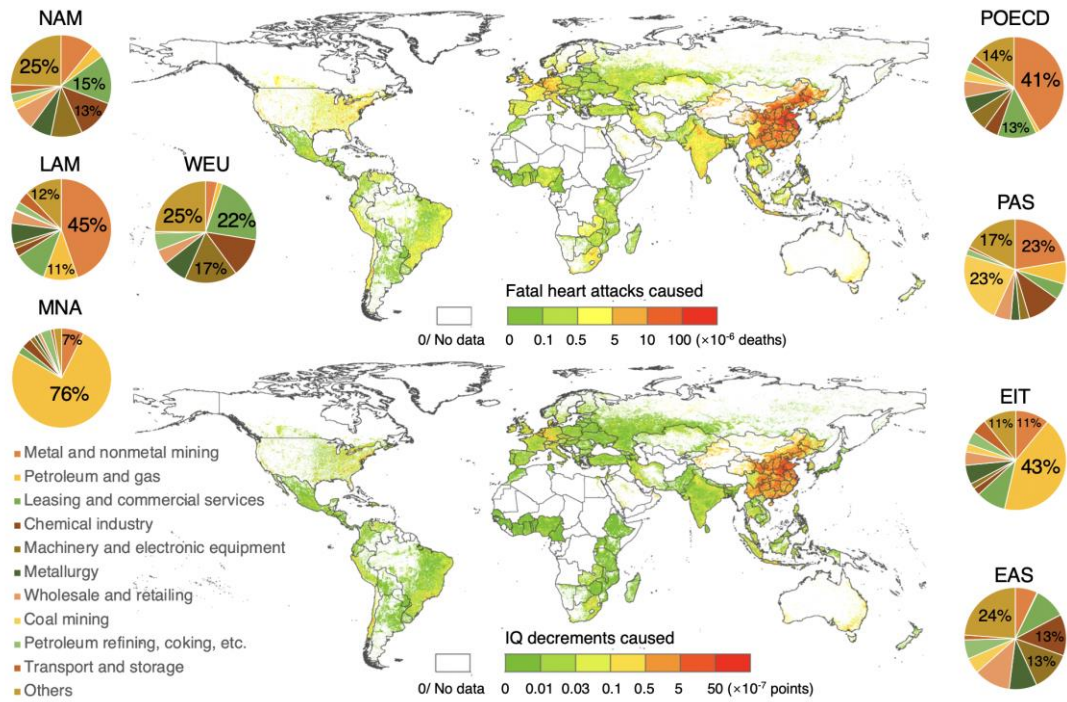
416 **3.3 Spatially explicit global primary suppliers enabling Hg-related health** 417 **impacts**

418 Figure 3 shows the spatially explicit global primary suppliers enabling China's
419 Hg-related human health impacts in 2010. Domestic primary inputs (mainly in Central
420 China, Northwest China, and North China) enable approximately 93% of the
421 Hg-related health impacts in China, while foreign primary inputs (mainly in North
422 America, Western Europe, and Japan) enable the remaining 7% of impacts (SI Figure
423 S8). For relatively developed regions such as the Central Coast, major sectoral source
424 enabling China's Hg-related health impacts is the *scientific research and other*

425 *services* sector. For the Northwest with abundant mineral resources, primary inputs in
426 the *metallurgy* sector takes the leading role. In the Central, primary inputs in the
427 *nonmetal products* sector contributes the most to Hg-related health impacts in China
428 (SI Figure S3). Foreign primary suppliers enabling significant Hg-related health
429 impacts in China involve the Pacific-OECD-1990 nations (including Australia, Japan,
430 and New Zealand), Latin America and the Caribbean, and the Middle East and North
431 Africa. See section S2 of the SI for more international and intranational trade pairs
432 inducing China's Hg-related health impacts. In particular, Australia is the largest
433 primary supplier, enabling 1.6×10^{-3} points of IQ decrements and 85 deaths from fatal
434 heart attacks in China. The *metal and nonmetal mining* sector and *petroleum and gas*
435 sector are the major sectoral sources for foreign primary suppliers. The *metal and*
436 *nonmetal mining* sector contributes nearly 50% of China's Hg-related health impacts
437 enabled by primary inputs of Pacific-OECD-1990 nations, as well as Latin America
438 and the Caribbean. The *petroleum and gas* sector contributes 76% for the Middle East
439 and North Africa. The reason is that China imports large amounts of mineral
440 resources from Australia and Latin America, and oil and gas resources from the
441 Middle East.⁴⁹

442 Figure 3 also shows a significant spatial heterogeneity in global primary suppliers
443 enabling Hg-related health impacts in China. The distribution of global primary
444 suppliers is significantly influenced by the distribution of resources, including mineral,
445 oil, gas, and water resources. Similarly, we provide a spatially explicit map of
446 domestic primary suppliers in China driving Hg-related health impacts (SI Figure S9).

447 In China, the resource-based distribution feature is obvious for hotspots in the Central
448 (e.g., Henan), North (e.g., Hebei, and Shanxi), and Northwest (e.g., Shaanxi, Gansu,
449 and Inner Mongolia). These regions have abundant fossil fuel and mineral resources
450 (e.g., coal in Shanxi and Inner Mongolia, nonferrous metals in Henan and Hebei, and
451 oil in Xinjiang). They provide raw materials to downstream producers and enable
452 downstream Hg-related health impacts. There are also hotspots in the Yangtze River
453 and Yellow River catchments driven by the availability of water resources. Moreover,
454 hotspots in Jiangsu Province have a distinct distribution feature along the Yangtze
455 River and Taihu Lake. For the rest of the world, hotspots also have obvious
456 characteristics of resource-based distributions. For example, hotspots in the Middle
457 East are associated with the distribution of oil fields along the Persian Gulf. Southeast
458 Asia is abundant in minerals, including coal mines in Vietnam and large gold mines in
459 Indonesia.⁵⁰ Thus, primary inputs in the *coal mining* and *metal and nonmetal mining*
460 sectors are major hotspot sources in Southeast Asia. The distribution of foreign
461 primary suppliers is also influenced by water resources (e.g., the Nile in Egypt, the
462 Amazon in northern Latin America, and the Rhine in Germany).



463

464 **Figure 3. Spatially explicit global primary suppliers enabling China's Hg-related**
 465 **health impacts in 2010.** Abbreviations: NAM – North America; LAM – Latin
 466 America and the Caribbean; WEU – Western Europe; MNA – the Middle East and
 467 North Africa; PAS – Southeast Asia and the Pacific; POECD – Pacific-OECD-1990
 468 nations (including Japan, Australia, and New Zealand); EIT – Economies in
 469 Transition (including Eastern Europe and the former Soviet Union); EAS – East Asia
 470 (China excluded).

471

472 In addition, many hotspots of primary suppliers are distributed based on urban
 473 agglomerations, dominated by the service industries. The *leasing and business*
 474 *services* sector in Beijing-Tianjin Region, Chengdu-Chongqing District, North
 475 America and Western Europe provides leasing and business services to downstream
 476 production activities and enables large Hg-related health impacts in China through
 477 global supply chains. Moreover, hotspots in the east coast of Australia and the
 478 northeast and west coasts of Latin America form the transportation-oriented

479 distribution. Hotspots in coastal areas provide transportation services to downstream
480 producers and enable large Hg-related health impacts in China through global supply
481 chains. This indicates the significant role of transportation in the distribution of
482 primary suppliers.

483 **4. IMPLICATIONS**

484 This study constructs a SEGTHI model, which integrates global economic supply
485 chains with China's biogeochemical Hg cycle. We map China's Hg-related health
486 impacts, associated global final consumers, and global primary suppliers at a high
487 spatial resolution. We observed significant spatial heterogeneity in hotspots of China's
488 Hg-related health impacts and global supply chain drivers. Results show that
489 approximately 1% of the land area holds 40% of the population but nearly 70% of the
490 fatal heart attack deaths in China. This indicates that the distribution of hotspots may
491 be influenced by many factors, such as economy, transportation, resources, and
492 dietary intake habits, not just the population density. This finer-scale study can help
493 more accurately locate the hotspots of Hg-related health impacts and economic
494 activities. It can facilitate more targeted policy decisions for the implementation of the
495 *Minamata Convention*.

496 **Comparisons with previous studies.** We compared our results with previous studies.
497 Compared with the gridded Hg emissions in China in 2010⁵¹, we find that Hg
498 emissions in the southeast coastal areas are relatively low, but their Hg-related health
499 impacts are relatively high. This is related to the high consumption of marine fish in

500 coastal areas and also reflects the Hg outflow from inland areas to coastal areas
501 through atmospheric transport. Conversely, Hg emissions in Henan province are high,
502 but the Hg-related health impacts are not so serious. This may explain the role of
503 atmospheric Hg transport and may be related to the low-rice and high-wheat dietary
504 habit in Henan province. The consumption of rice is one of the most important
505 pathways to MeHg exposure.²⁵

506 Moreover, compared with our previous study, spatially explicit results help
507 identify the specific sources and distribution of global hotspots. They can guide more
508 accurate and effective measures to reduce Hg-related health impacts. Compared with
509 the sub-national results in our previous study, this study observed many areas where
510 Hg-related health impacts are overestimated or underestimated (SI Figure S12). For
511 example, the total Hg-related health impacts in Beijing, Tianjin, and Shanghai are
512 relatively low. However, they have many spatially explicit hotspots of Hg-related
513 health impacts. In addition, the total Hg-related health impacts in Hebei and Shandong
514 are not much high. However, special attention should be paid to Shijiazhuang,
515 Tangshan, Jinan, and other industrial cities, because of their large Hg emissions and
516 high Hg-related health impacts. On the other hand, although the total Hg-related
517 health impacts in Jiangsu, Zhejiang, Guangdong, and Sichuan are relatively high,
518 most of the hotspots in these regions are concentrated in limited areas including the
519 Yangtze River Delta, Pearl River Delta, and Chengdu-Chongqing District. The
520 spatially explicit findings of this study can support the successful implementation of
521 the *Minamata Convention* from two aspects: providing spatially explicit hotspots for

522 policy decisions in various stages of global supply chains and for international
523 cooperation.

524 **Spatially explicit policy implications.** Three perspectives are widely recognized to
525 identify hotspots of global supply chains, comprising production-side, demand-side,
526 and supply-side perspectives. Production-side control measures are effective for Hg
527 emissions and related health impact hotspots, including improving energy use
528 efficiency, promoting low-Hg energy sources, and establishing Hg removal facilities.⁵²
529 Spatially explicit measures should focus on hotspots including power plants in the
530 Yangtze River Delta and Pearl River Delta, the *nonmetal products* sectors of urban
531 agglomerations in the middle reaches of the Yangtze River (especially in Wuhan,
532 Changsha, and Nanchang), and the *metallurgy* sector in certain large mining areas.

533 Demand-side control measures, mainly aiming at the optimization of consumption
534 behaviours through economic instruments, are effective in hotspot areas where the
535 final demand induces significant upstream health impacts through global supply
536 chains.⁵³ According to the results of this study, consumption behaviour optimization
537 should focus on the *construction* sector in the urban agglomerations of
538 Beijing-Tianjin Region, Middle-Lower Yangtze River, and Pearl River Delta in China.
539 For foreign hotspots, relevant measures should be aimed at the eastern U.S. (mainly
540 New York, Boston, Washington D.C., and Chicago), Cologne and Munich in
541 Germany, and London and Manchester in the United Kingdom. Moreover, the
542 demand and productivity of construction activities in Saudi Arabia should be
543 concerned.

544 Supply-side measures, focusing on the optimization of primary input behaviours
545 such as the adjustment of tax rates and financial incentives on selling low-Hg
546 products, are effective in critical geographic and sectoral sources whose primary
547 inputs enable large downstream health impacts.³⁵ Decision makers could limit loan
548 supply and subsidies to the *metal and nonmetal mining* and *metallurgy* sectors in the
549 coastal areas of Australia and Latin America (mainly in Brisbane, Melbourne, Rio de
550 Janeiro, and Santiago). For the Persian Gulf coast in the Middle East and the large oil
551 fields in Eastern Europe, authorities can choose to invest in dominant petroleum and
552 gas enterprises with less income-based Hg-related health impacts. In addition, primary
553 inputs of the *leasing and commercial services* sector in Western Europe (especially
554 southwest Germany) enable large amounts of Hg-related health impacts in China.
555 These regions could encourage their leasing and commercial enterprises to
556 preferentially serve enterprises with lower income-based Hg-related health impacts.

557 Different from previous studies, the findings of this study can identify spatially
558 explicit geographical and sectoral hotspots for the implementation of these three types
559 of measures. Considering the spatial heterogeneity of hotspots, control strategies
560 should be conducted in regions where hotspots are relatively concentrated (e.g.,
561 developed urban agglomerations). Notably, almost all of the Hg-related health
562 impacts in Sichuan are concentrated in its eastern part and connected with Chongqing.
563 Thus, measures in this region can only focus on Chengdu, Chongqing, and their
564 surrounding areas. This can significantly improve the effectiveness of measures
565 controlling Hg-related health impacts across the whole province. Moreover, some

566 hotspots distribute along the transportation arteries and large rivers, which are not
567 limited to administrative boundaries. Thus, the measures should consider
568 cross-boundary cooperation and may potentially be coordinated with city,
569 transportation, and resource management.

570 International cooperation is an important component of the *Minamata Convention*⁵.
571 The results of this study provide scientific foundations for this component by
572 identifying spatially explicit international trade pairs from the demand and supply
573 perspectives (SI S2). From the demand perspective, measures should focus on the
574 international pair of east-central U.S. and coastal areas in China (mainly the Yangtze
575 River Delta and Pearl River Delta). From the supply perspective, international
576 cooperation should focus on the interconnections between resource-exporting regions
577 and corresponding Chinese areas, such as coastal areas in Australia –
578 Chengdu-Chongqing District and the Middle East – Yangtze River Delta. Potential
579 measures include transferring technologies and related capital from these global
580 consumers and primary suppliers to hotspots of Hg-related health impacts in China.
581 For instance, dominant enterprises of the *metal and nonmetal mining* sector in the
582 coastal areas of southeastern Australia could transfer technologies and related capital
583 to the Chengdu-Chongqing District in China to reduce Hg-related health impacts there.
584 In addition, intranational cooperation is critical for reducing the overall Hg-related
585 health impacts in China. Herein, we find that Northwest (mainly in the Yellow River
586 Basin) – Southwest (mainly in Chengdu-Chongqing District) is an important trade

587 pair leading to the most Hg-related health impacts in China. Intranational cooperation
588 between these two regions should be promoted by national governments.

589 **Limitations and uncertainties.** The methods of this study have certain limitations.
590 On one hand, due to the limitation of computing resources and the lack of
591 high-resolution meteorological data, the resolution of this SEGTHI model is limited
592 by the horizontal resolutions in the chemical transport model. To analyze China's
593 Hg-related health impacts and the economic drivers at a higher spatial resolution, we
594 spatialize these factors based on certain regional heterogeneity features (e.g.,
595 population, socioeconomic status, food consumption, and income). Therefore, our
596 finer-scale model is a parametric model developed with multiple parameters. It can
597 reflect the influence of multiple factors, not just population. Specifically, we use the
598 gridded population data at the $1\text{km} \times 1\text{km}$ scale and city-level dietary intake data to
599 spatialize the production-based Hg-related health impacts in China, reflecting the
600 influence of population density and dietary intake. In terms of China's Hg-related
601 health impacts driven by global final demand and primary inputs, we use gridded data
602 of global nighttime lights and GDP at the $1\text{km} \times 1\text{km}$ scale as the proxy variables to
603 spatialize global final demand and primary inputs, respectively. This can reflect the
604 influence of socioeconomic factors and reveal the global economic drivers at a finer
605 scale than the national/subnational level. This study can reveal the spatially explicit
606 features of global final consumers and primary suppliers (e.g., city-level, basin-based,
607 and cross-boundary features of global economic drivers). Our SEGTHI model is
608 currently refined and improved at the output terminal of Hg-related health impacts,

609 while the front-end emission data and mid-end transport model are limited by the lack
610 of gridded data, computing resources, and the background of meteorological data. It is
611 difficult to unify the resolution of the whole model. Improving this limitation depends
612 on the refinement of Hg emission data and meteorological data. On the other hand, at
613 present, there are debates about whether Hg-related heart attacks are fatal. Some
614 scholars believe that MeHg intake may lead to deaths from fatal heart attacks, while
615 other scholars hold objections. Giang and Selin¹⁹ calculated both the non-fatal heart
616 attacks and fatal heart attacks in the U.S., while Chen et al.¹⁷ evaluated the deaths
617 from fatal heart attacks in China. According to the data availability, this study uses the
618 deaths from fatal heart attacks to characterize Hg-related health impacts.

619 This study is subject to certain uncertainties. Uncertainties mainly originate from
620 the estimations of China's atmospheric Hg emissions, global MRIO data, chemical
621 transport model simulations, the intake inventory of MeHg, and the evaluation of
622 human health impacts. We conducted a Monte Carlo simulation with 10,000 samples
623 of these factors. The P10 and P90 values of the statistical distributions are set as the
624 lower and upper limits of the uncertainty range. For example, ranges for the national
625 Hg-related health impacts of per-foetus IQ decrement points caused by atmospheric
626 Hg emissions from Central China are $(0.39 \times 10^{-2}, 4.31 \times 10^{-2})$. For deaths from fatal
627 heart attacks, the uncertainties are estimated at (433, 2693). The uncertainties in the
628 points of per-foetus IQ decrements and deaths from fatal heart attacks driven by the
629 final demand of the U.S. are $(0.06 \times 10^{-2}, 0.61 \times 10^{-2})$ and (70, 374). From the supply
630 perspective, the uncertainties enabled by the primary inputs of Australia are

631 (0.03×10⁻², 0.30×10⁻²) and (35, 182). See SI S3 for more details of the uncertainties,
632 including the specific sources and related improvement measures.

633 **AUTHOR CONTRIBUTIONS**

634 Conceptualization, S.L.; Methodology, S.L., Y.L., L.C., and J.Q.; Investigation, Y.L.,
635 L.C., J.Q., and H.Z.; Writing and revisions, all authors; Supervision, S.L.

636 **COMPETING INTERESTS**

637 The authors declare no competing interests.

638 **ACKNOWLEDGEMENTS**

639 This study is financially supported by the National Natural Science Foundation of
640 China (71874014 and 41701589).

641 **SUPPORTING INFORMATION**

642 Additional information on (1) the complete methods and data sources (S1); (2)
643 international and intranational trade inducing Hg-related health impacts in China (S2);
644 (3) the limitations and uncertainties of this study (S3); (4) supplementary data and
645 results (S4, Figures S4-S12); (6) the list of aggregated Chinese and world regions, as
646 well as regions in the GATP 9 Database (Tables S1 and S2). This information is
647 available free of charge via the Internet at <http://pubs.acs.org>.

648 **REFERENCES**

649 1. Driscoll, C. T.; Mason, R. P.; Chan, H. M.; Jacob, D. J.; Pirrone, N. Mercury as a
650 global pollutant: sources, pathways, and effects. *Environ. Sci. Technol.* **2013**, *47*,
651 4967-4983.

- 652 2. Selin, N. E. Global biogeochemical cycling of mercury: a review. *Ann. Rev.*
653 *Environ. Resources* **2009**, *34*, 43-63.
- 654 3. WHO. Mercury and health: Key facts;
655 <https://www.who.int/en/news-room/fact-sheets/detail/mercury-and-health>.
- 656 4. Lavoie, R. A.; Jardine, T. D.; Chumchal, M. M.; Kidd, K. A.; Campbell, L. M.
657 Biomagnification of mercury in aquatic food webs: a worldwide meta-analysis.
658 *Environ. Sci. Technol.* **2013**, *47*, 13385-13394.
- 659 5. UNEP. *Minamata Convention on Mercury*; United Nations Environment
660 Programme: Geneva, Switzerland, 2013.
- 661 6. Lin, Y.; Wang, S. X.; Steindal, E. H.; Wang, Z. G.; Braaten, H. F. V.; Wu, Q. R.;
662 Larssen, T. A Holistic Perspective Is Needed To Ensure Success of Minamata
663 Convention on Mercury. *Environ. Sci. Technol.* **2017**, *51*, 1070-1071.
- 664 7. Axelrad, D. A.; Bellinger, D. C.; Ryan, L. M.; Woodruff, T. J. Dose-response
665 relationship of prenatal mercury exposure and IQ: an integrative analysis of
666 epidemiologic data. *Environ. Health Perspect.* **2007**, *115*, 609-615.
- 667 8. Mahaffey, K. R.; Clickner, R. P.; Bodurow, C. C. Blood organic mercury and
668 dietary mercury intake: National Health and Nutrition Examination Survey, 1999
669 and 2000. *Environ. health perspect.* **2003**, *112*, 562-570.
- 670 9. Myers, G. J.; Davidson, P. W.; Cox, C.; Shamlaye, C. F.; Palumbo, D.;
671 Cernichiari, E.; Sloane-Reeves, J.; Wilding, G. E.; Kost, J.; Huang, L.-S.;
672 Clarkson, T. W. Prenatal methylmercury exposure from ocean fish consumption
673 in the Seychelles child development study. *The Lancet* **2003**, *361*, 1686-1692.
- 674 10. Roman, H. A.; Walsh, T. L.; Coull, B. A.; Dewailly, É.; Guallar, E.; Hattis, D.;
675 Mariën, K.; Schwartz, J.; Stern, A. H.; Virtanen, J. K.; Rice, G. Evaluation of the
676 cardiovascular effects of methylmercury exposures: current evidence supports
677 development of a dose-response function for regulatory benefits analysis.
678 *Environ. Health Perspect.* **2011**, *119*, 607-614.
- 679 11. Pirrone, N.; Cinnirella, S.; Feng, X.; Finkelman, R. B.; Friedli, H. R.; Leaner, J.;
680 Mason, R.; Mukherjee, A. B.; Stracher, G. B.; Streets, D. G.; Telmer, K. Global
681 mercury emissions to the atmosphere from anthropogenic and natural sources.
682 *Atmos. Chem. Phys.* **2010**, *10*, 5951-5964.
- 683 12. Pacyna, E. G.; Pacyna, J. M.; Sundseth, K.; Munthe, J.; Kindbom, K.; Wilson, S.;
684 Steenhuisen, F.; Maxson, P. Global emission of mercury to the atmosphere from
685 anthropogenic sources in 2005 and projections to 2020. *Atmos. Environ.* **2010**,
686 *44*, 2487-2499.
- 687 13. Streets, D. G.; Hao, J.; Wu, Y.; Jiang, J.; Chan, M.; Tian, H.; Feng, X.
688 Anthropogenic mercury emissions in China. *Atmos. Environ.* **2005**, *39*,
689 7789-7806.
- 690 14. Chen, L.; Meng, J.; Liang, S.; Zhang, H.; Zhang, W.; Liu, M.; Tong, Y.; Wang,
691 H.; Wang, W.; Wang, X.; Shu, J. Trade-induced atmospheric mercury deposition
692 over China and implications for demand-side controls. *Environ. Sci. Technol.*
693 **2018**, *52*, 2036-2045.
- 694 15. Liu, M.; Chen, L.; Wang, X.; Zhang, W.; Tong, Y.; Ou, L.; Xie, H.; Shen, H.; Ye,
695 X.; Deng, C.; Wang, H. Mercury Export from Mainland China to Adjacent Seas

- 696 and Its Influence on the Marine Mercury Balance. *Environ. Sci. Technol.* **2016**,
697 *50*, 6224-6232.
- 698 16. Clayden, M. G.; Kidd, K. A.; Wyn, B.; Kirk, J. L.; Muir, D. C. G.; Odriscoll, N.
699 J. Mercury biomagnification through food webs Is affected by physical and
700 chemical characteristics of lakes. *Environ. Sci. Technol.* **2013**, *47*, 12047-12053.
- 701 17. Chen, L.; Liang, S.; Liu, M.; Yi, Y.; Mi, Z.; Zhang, Y.; Li, Y.; Qi, J.; Meng, J.;
702 Tang, X.; Zhang, H.; Tong, Y.; Zhang, W.; Wang, X.; Shu, J.; Yang, Z.
703 Trans-provincial health impacts of atmospheric mercury emissions in China. *Nat.*
704 *Commun.* **2019**, *10*, 1484.
- 705 18. Sunderland, E. M.; Li, M.; Bullard, K. Decadal Changes in the Edible Supply of
706 Seafood and Methylmercury Exposure in the United States. *Environ. health*
707 *perspect.* **2018**, *126*, 029003.
- 708 19. Giang, A.; Selin, N. E. Benefits of mercury controls for the United States. *Proc.*
709 *Natl. Acad. Sci. U. S. A.* **2016**, *113*, 286-291.
- 710 20. Wu, Q.; Li, G.; Wang, S.; Liu, K.; Hao, J. Mitigation options of atmospheric Hg
711 emissions in China. *Environ. Sci. Technol.* **2018**, *52*, 12368-12375.
- 712 21. Hui, M.; Wu, Q.; Wang, S.; Liang, S.; Zhang, L.; Wang, F.; Lenzen, M.; Wang,
713 Y.; Xu, L.; Lin, Z.; Yang, H.; Lin, Y.; Larssen, T.; Xu, M.; Hao, J. Mercury
714 flows in China and global drivers. *Environ. Sci. Technol.* **2017**, *51*, 222-231.
- 715 22. Qi, J.; Wang, Y. F.; Liang, S.; Li, Y.; Li, Y. M.; Feng, C. Y.; Xu, L. X.; Wang, S.
716 X.; Chen, L.; Wang, D. F.; Yang, Z. F. Primary suppliers driving atmospheric
717 mercury emissions through global supply chains. *One Earth* **2019**, *1*, 254-266.
- 718 23. Angot, H.; Hoffman, N.; Giang, A.; Thackray, C. P.; Hendricks, A. N.; Urban,
719 N.; Selin, N. E. Global and local impacts of delayed mercury mitigation efforts.
720 *Environ. Sci. Technol.* **2018**, *52*, 12968-12977.
- 721 24. UNEP. *Global Mercury Assessment 2018*. United Nations Environment
722 Programme: Geneva, Switzerland, 2019.
- 723 25. Zhang, H.; Feng, X.; Larssen, T.; Qiu, G.; Vogt, R. D. In inland China, rice,
724 rather than fish, is the major pathway for methylmercury exposure. *Environ.*
725 *Health Perspect.* **2010**, *118*, 1183-1188.
- 726 26. Feng, X.; Li, P.; Qiu, G.; Wang, S.; Li, G.; Shang, L.; Meng, B.; Jiang, H.; Bai,
727 W.; Li, Z. Human exposure to methylmercury through rice intake in mercury
728 mining areas, Guizhou Province, China. *Environ. Sci. Technol.* **2008**, *42*,
729 326-332.
- 730 27. Liang, S.; Zhang, C.; Wang, Y.; Xu, M.; Liu, W. Virtual atmospheric mercury
731 emission network in China. *Environ. Sci. Technol.* **2014**, *48*, 2807-2815.
- 732 28. National Statistics Bureau of China, *Sample Survey of 1% of population in China*,
733 *2015*; China Statistics Press: Beijing, 2016.
- 734 29. Wiedmann, T. O.; Schandl, H.; Lenzen, M.; Moran, D.; Suh, S.; West, J.;
735 Kanemoto, K. The material footprint of nations. *Proc. Natl. Acad. Sci. U. S. A.*
736 **2015**, *112*, 6271-6276.
- 737 30. Wang, H.; Zhang, Y.; Zhao, H.; Lu, X.; Zhang, Y.; Zhu, W.; Nielsen, C. P.; Li,
738 X.; Zhang, Q.; Bi, J. Trade-driven relocation of air pollution and health impacts
739 in China. *Nat. Commun.* **2017**, *8*, 738-738.

- 740 31. Liang, S.; Wang, Y.; Cinnirella, S.; Pirrone, N. Atmospheric mercury footprints
741 of nations. *Environ. Sci. Technol.* **2015**, *49*, 3566-3574.
- 742 32. Mi, Z. F.; Meng, J.; Guan, D. B.; Shan, Y. L.; Song, M. L.; Wei, Y. M.; Liu, Z.;
743 Hubacek, K. Chinese CO₂ emission flows have reversed since the global
744 financial crisis. *Nat. Commun.* **2017**, *8*, 1712.
- 745 33. Peters, G. P. From production-based to consumption-based national emission
746 inventories. *Ecol. Econ.* **2008**, *65*, 13-23.
- 747 34. Miller, R. E.; Blair, P. D. *Input-Output Analysis: Foundations and Extensions*. 2
748 ed.; Cambridge Univ. Press: Cambridge, 2009.
- 749 35. Liang, S.; Qu, S.; Zhu, Z.; Guan, D.; Xu, M. Income-Based Greenhouse Gas
750 Emissions of Nations. *Environ. Sci. Technol.* **2017**, *51*, 346-355.
- 751 36. Marques, A.; Rodrigues, J. F. D.; Lenzen, M.; Domingos, T. Income-based
752 environmental responsibility. *Ecol. Econ.* **2012**, *84*, 57-65.
- 753 37. Liu, M.; Chen, L.; He, Y.; Baumann, Z.; Mason, R. P.; Shen, H.; Yu, C.; Zhang,
754 W.; Zhang, Q.; Wang, X. Impacts of farmed fish consumption and food trade on
755 methylmercury exposure in China. *Environ. Int.* **2018**, *120*, 333-344.
- 756 38. Rice, G. E.; Hammitt, J. K.; Evans, J. S. A Probabilistic Characterization of the
757 Health Benefits of Reducing Methyl Mercury Intake in the United States.
758 *Environ. Sci. Technol.* **2010**, *44*, 5216-5224.
- 759 39. Xu, X. *1km*1km grid data collection of population in China*. 2017.
760 <http://www.resdc.cn/DOI>.
- 761 40. National Statistics Bureau of China, *China Statistical Yearbook, 2010*. China
762 Statistics Press: Beijing, 2011.
- 763 41. NCEI. *Version 4 DMSP-OLS Nighttime Lights*. National Centers for
764 Environmental Information, 2010.
765 <https://www.ngdc.noaa.gov/eog/dmsp/downloadV4composites.html>.
- 766 42. Henderson, J. V.; Storeygard, A.; Weil, D. N. A Bright Idea for Measuring
767 Economic Growth. *The American Econ. Rev.* **2011**, *101*, 194-199.
- 768 43. UNEP/DEWA/GRID-Geneva. *Gross Domestic Product 2010*.
769 <https://preview.grid.unep.ch/index.php?preview=data&events=socec&evcat=1&lang=eng>.
- 770
- 771 44. Li, C.; Wang, A.; Chen, X.; Chen, Q.; Zhang, Y.; Li, Y. Regional distribution
772 and sustainable development strategy of mineral resources in China. *Chin. Geogr.*
773 *Sci.* **2013**, *23*, 470-481.
- 774 45. Yu, C. China's water crisis needs more than words. *Nature* **2011**, *470*, 307.
- 775 46. Henders, S.; Persson, U. M.; Kastner, T. Trading forests: land-use change and
776 carbon emissions embodied in production and exports of forest-risk commodities.
777 *Environ. Res. Lett.* **2015**, *10*, 125012.
- 778 47. Taylor, G. S. Top 10 states for manufacturing 2019. *Global Trade*, Sep 2, 2019,
779 <https://www.globaltrademag.com/top-10-states-for-manufacturing-2019/>.
- 780 48. USDT, *State Transportation Statistics 2010*. United States Department of
781 Transportation. **2010**, <https://www.bts.gov/ctp>.
- 782 49. General Administration of Customs of the People's Republic of China, *China*
783 *Custons Statistical Yearbook, 2010*; China Customs Press: Beijing, 2011.

- 784 50. Pombhejara, V. n. 8 - Natural Resources and Raw Materials in Southeast Asia. In
785 *Asia and the New International Economic Order*; Jorge A. Lozoya and A.K.
786 Bhattacharya, Eds.; Elsevier 1981; pp 164-173.
- 787 51. Zhang, L.; Wang, S.; Wang, L.; Wu, Y.; Duan, L.; Wu, Q.; Wang, F.; Yang, M.;
788 Yang, H.; Hao, J.; Liu, X. Updated emission inventories for speciated
789 atmospheric mercury from anthropogenic sources in China. *Environ. Sci.*
790 *Technol.* **2015**, *49*, 3185-3194.
- 791 52. Wu, Q.; Wang, S.; Liu, K.; Li, G.; Hao, J. Emission-Limit-Oriented Strategy To
792 Control Atmospheric Mercury Emissions in Coal-Fired Power Plants toward the
793 Implementation of the Minamata Convention. *Environ. Sci. Technol.* **2018**, *52*,
794 11087-11093.
- 795 53. Liang, S.; Xu, M.; Liu, Z.; Suh, S.; Zhang, T. Socioeconomic drivers of mercury
796 emissions in China from 1992 to 2007. *Environ. Sci. Technol.* **2013**, *47*,
797 3234-3240.

798